This is an preprint of an article published in International Journal of Heat and Mass Transfer 52 (11-12) 2543-2551 (2009).
DOI: http://dx.doi.org/10.1016/j.ijheatmasstransfer.2008.11.022.

Impact of Marangoni instabilities on the fluid dynamic behaviour of organic droplets

M. Wegener*, M. Fevre, A.R. Paschedag+, M. Kraume

Chair of Chemical Engineering, Technische Universität Berlin, Ackerstraße 71-76, D-13355 Berlin, Germany

+ *University of Applied Science Berlin, Luxemburger Str. 10, D-13353 Berlin, Germany*

Abstract

Marangoni instabilities in dispersed liquid/liquid systems occur if the local solute concentration varies over the interface. The additional shear stress at the interface between a droplet and an ambient phase generates complex convection patterns which increase temporarily the global drag coefficient of the drop and thus retard the drop rise velocity. When Marangoni effects get weaker, the shear forces decrease and the drop reaccelerates. In the present experimental study, the transient drop rise velocity has been intensely investigated in the system toluene$_{(d)}$/acetone$_{(s)}$/water$_{(c)}$ for different initial solute concentrations and different drop diameters. Both mass transfer directions have been considered. The reacceleration time as an indicator of the end of Marangoni dominance can be expressed as a function of drop diameter and initial solute concentration.

Keywords: droplet, solvent extraction, Marangoni convection, mass transfer

Nomenclature

c	concentration (g/L)
C_D	drag coefficient
d	diameter (m)
f	frequency (Hz)
m	distribution coefficient (-)
P	power (W)
R^2	correlation coefficient
t	time (s)
v	drop velocity (m/s)
x	vertical coordinate (m)
y	horizontal coordinate (m)

Greek symbols

μ	dynamic viscosity (Pa·s)
μ^*	viscosity ratio μ_d/μ_c
ρ	density (kg/m^3)
σ	interfacial tension (N/m)

* Corresponding author. Tel.: +49 30 314 72791; fax: +49 30 314 21134.
E-mail addresses: mirco.wegener@tu-berlin.de (M. Wegener),
anja.paschedag@tfh-berlin.de (A.R. Paschedag),
matthias.kraume@tu-berlin.de (M. Kraume).

This is an preprint of an article published in International Journal of Heat and Mass Transfer 52 (11-12) 2543-2551 (2009).
DOI: http://dx.doi.org/10.1016/j.ijheatmasstransfer.2008.11.022. © copyright 2009 Elsevier Ltd.

Dimensionless numbers

Re	Reynolds number $\frac{v_t d_P \rho_c}{\mu_c}$

Subscripts

0	initial
∞	infinity
c	continuous phase
d	dispersed phase
fi	freely moving interface
hi	high
I	interface
lo	low
P	particle, drop
r	radial coordinate
R	drop radius
rs	rigid sphere
s	solute
t	terminal

This is an preprint of an article published in International Journal of Heat and Mass Transfer 52 (11-12) 2543-2551 (2009).
DOI: http://dx.doi.org/10.1016/j.ijheatmasstransfer.2008.11.022.

1. Introduction

The design of liquid-liquid extraction columns is in many cases a very time consuming and expensive task since preliminary tests in pilot plants are necessary to deduce the relevant information, e.g. mass transfer coefficients and residence times of the droplet population. A reliable prediction of the important parameters is a challenging issue due to the manifold interactions in a dispersed liquid/liquid system. For example, the determination of the mass transfer coefficient is only possible if the total surface area available for mass transfer is known, i.e. via the drop size distribution. The latter depends mainly on the two competitive mechanisms breakage and coalescence which in turn are determined by a complex list of physical and geometrical parameters. Additionally, interfacial phenomena as drop deformation and oscillation, the adsorption of surfactants at the interface of the droplets or the presence of Marangoni convection due to local temperature or concentration gradients strongly affect the mass transfer coefficient and also hydrodynamic parameters like the terminal drop velocity.

Particularly the Marangoni effects are of interest since interfacial instabilities are able to promote mass transfer significantly [1, 2]. Local variations in the solute concentration occur usually if mass transfer is present and lead to interfacial tension gradients or more general to gradients in the chemical potential [3] at the interface if the interfacial tension σ is a function of the solute concentration, i.e. if $\sigma = f(c_{s,I})$. An interfacial flow is induced because the system tends to lower its free energy in expanding regions of low interfacial tension (Marangoni effect) which in consequence affects both phases adjacent to the interface (see Fig. 1). Thus, the velocity field inside and in the immediate vicinity of the drop is influenced by these instabilities. As a consequence, since the concentration field is coupled with the velocity field via the convective terms in the species balance, the concentration field is affected as well. The change in mass transfer, finally, affects the local solute concentration at the interface and thus the gradient of interfacial tension.

Position of Fig. 1

Up to now it is not possible to predict reliably the appearance of such interfacial instabilities for a given liquid/liquid dispersion. In order to analyse processes at the interface in a detailed way, the complex polydispersed system is often reduced to a single drop and its ambient flow. In this study we will focus on the impact of interfacial instabilities on the hydrodynamic behaviour of a single rising droplet in a quiescent continuous phase. Previous studies confirmed that the transient drop rise velocity is highly sensitive to Marangoni induced shear stresses exerted at the interface as shown by Henschke [4], Schulze & Kraume [5] and recently by Wegener et al. [6] in systems with solute transfer but without added surfactants. These tangential flows at the interface are of arbitrary direction and thus lower the relative velocity between dispersed and ambient phase, in other words: the overall drag coefficient is temporarily increased. In fact, if the initial solute concentration is high enough, Marangoni convection can be so strong that internal circulation is hindered due to the “blockage effect” of the tangential flows. On a macroscopic level, the drop behaves transitorily like a rigid sphere, but on a microscopic scale chaotic flow structures inside and outside the drop occur. As mass transfer goes on, Marangoni convection becomes weaker due to the reduction of the concentration gradients. Thus, the shear stresses opposing the

This is an preprint of an article published in International Journal of Heat and Mass Transfer 52 (11-12) 2543-2551 (2009).
DOI: http://dx.doi.org/10.1016/j.ijheatmasstransfer.2008.11.022. © copyright 2009 Elsevier Ltd.

ambient flow decrease and the relative velocity between both phases can increase. Eventually, the internal circulation starts and the drop reaccelerates.

The rise or fall of drops in liquid media are subject to numerous works performed in the past. In terms of fluid dynamics, the key issue was to predict the terminal velocity or the drag coefficient respectively as a function of the equivalent drop diameter for a given system.

Role of impurities and surfactants on the drag

Hu & Kintner [7] performed investigations on various organic liquid drops falling in water. They proposed an empirical correlation for the drag coefficient covering a wide range of physical properties. For non-oscillating particles, the drag coefficient was equal to that of a comparable rigid sphere. The data suggest that the systems were contaminated and thus no internal circulation could develop. For Reynolds numbers higher than 300, a sharp increase in the drag due to shape oscillation was found. Johnson & Braida [8] reported drag coefficients for drops on the rigid sphere curve as well. They proposed a modified correlation based closely to the Hu & Kintner correlation. Licht & Narasimhamurty [9] published their work on the rate of fall of single drops at the same time as Hu & Kintner. Four of the systems were identical, but significantly higher fall velocities could be found which was mainly attributed to the quality of the used chemicals and the chemical resistance of the used materials. Thorsen et al. [10] and Edge & Grant [11] compared own experimental data with the correlation of Hu & Kintner. They found good agreement when the system was contaminated, obvious disagreement was stated for purified systems. Griffith [12] investigated the effect of surfactants on the terminal velocity of drops. Surfactants adsorb at the interface and are transported to the rear of the drop where they form a stagnant cap. In the vicinity of the stagnant cap, a gradient in interfacial tension occurs which leads to an interfacial flow, and thus shear stress opposes the viscous stress exerted on the interface by the ambient liquid. It follows a retardation of the drop. Mekasut et al. [13] made similar observations in a different system. With higher amounts of surfactant the drop rise velocity decreases in the whole diameter range investigated.

Internal circulation

A technique to visualize internal drop motion was presented by Spells [14]. In a more recent work by Amar et al. [15], the NMR technique (nuclear magnetic resonance spectroscopy) was utilised to visualize the circulation inside droplets. Garner & Skelland [16] showed in their experiments that the fall velocities were the higher the more vigorous the internal circulations were. They stated that drops were falling up to 40% faster than a comparable rigid sphere in some cases. Klee & Treybal [17] confirmed in own experiments that internal circulation reduces the drag coefficient. For every system the drag coefficient was found to be smaller than for the comparable rigid sphere in the non-oscillating regime. They proposed a new correlation for the terminal velocity which shows good agreement with experimental data. Elzinga & Banchero [18] reported drag coefficients for several liquid/liquid systems. They emphasized the importance of higher internal circulation in referring to heat transfer measurements where the heat transfer coefficient was larger for uncontaminated drops. Additionally, they observed in shadowgraphs a shift of the point of boundary layer separation to the rear stagnation point which is believed to cause the decrease in the drag coefficient. Winnikow & Chao [19] presented in their study an estimation for the separation angle. Boundary layer separation and internal circulation were demonstrated

This is an preprint of an article published in International Journal of Heat and Mass Transfer 52 (11-12) 2543-2551 (2009).
DOI: http://dx.doi.org/10.1016/j.ijheatmasstransfer.2008.11.022. © copyright 2009 Elsevier Ltd.

also using shadowgraphs. Again, the system purity was believed to be responsible for lower drag coefficients.

Effect of simultaneous mass transfer

Keith and Hixson [20] provided data for the velocities of toluene drops in water loaded with different types of solutes. The presence of solutes changed significantly the drop rise velocity compared to unloaded toluene drops, but the authors gave no further explanation on this issue, especially on the fact if mass transfer was completed or not when the velocity measurement was accomplished. In the same system toluene/acetone/water, Al-Hassan et al. [21] observed an increase in the drag coefficient for large oscillating drops when there was solute mass transfer. Linde & Sehrt [22] showed in their experiments in the system benzaldehyde/acetic acid/water that the increase of the fluid dynamic resistance is a function of the mass transfer direction and solute concentration. They concluded that inner circulation is hindered due to local limited and primary tangential flows at the interface. Sawistowski [2] observed in a nitrobenzene/propionic acid/water system that the drag coefficient depends also on the mass transfer direction. Henschke & Pfennig [23] and in more detail Henschke [4] discussed the effect of mass transfer induced instabilities on the movement of the interface for several systems. The inner chaotic flow patterns lead to an increase in the shear stress at the interface and thus to a retardation of the drop rise velocity. Garthe [24] observed that the reduction in the drop rise velocity can possibly depend on the mass transfer direction. In the toluene/acetone/water system no significant effect could be stated, whereas in the butylacetate/acetone/water system drops were faster when the mass transfer was from the continuous phase to the organic droplets.

Scope of this study

The aim of the present study is to investigate the impact of simultaneous mass transfer on the drop rise velocity in the system toluene/acetone/water without any added surfactants. The drop rise velocity shows a characteristic acceleration behaviour which indicates the presence and strength of solutal Marangoni convection at the interface. It will be shown that the duration of Marangoni effects depends on the parameters initial solute concentration, mass transfer direction and drop diameter. The initial solute concentrations are varied in the range from 0.9 to 95 g/L, the range of drop diameters is between 1 and 2.5 mm. A graphical correlation will be given in order to predict the reacceleration time which can be regarded as the end of Marangoni convection dominance.

2. Experimental detail

2.1 Experimental setup

Fig. 2 shows a scheme of the experimental setup, consisting of the test column (1) and the peripheral devices. The column (diameter 75 mm, height 1000 mm) is made of borosilicate glass (Schott®). A jacket (2) is mounted around the column, filled with anhydrous glycerol to allow for temperature control (temperature is set to 25°C) and undistorted optical access since the refractive indices of borosilicate glass and glycerol are nearly equal. The glycerol is circulated by a gear pump (3) through the thermostat (4) (RK 20 by Lauda®) in a separate loop.

This is an preprint of an article published in International Journal of Heat and Mass Transfer 52 (11-12) 2543-2551 (2009).
DOI: http://dx.doi.org/10.1016/j.ijheatmasstransfer.2008.11.022. © copyright 2009 Elsevier Ltd.

For the measurements, the standard test system toluene$_{(d)}$/acetone$_{(s)}$/water$_{(c)}$ (*d*: dispersed phase, *s*: solute, *c*: continuous phase) as recommended by the European Federation of Chemical Engineering [25] has been used. The relevant physical properties are given in [25] as well. Since the behaviour of toluene droplets is highly sensitive to impurities and quality of the chemicals, only chemicals of high purity have been used (toluene p.a. ≥ 99.9 %, acetone p.a. ≥ 99.8 % by Merck®, deionized water with a specific resistance of 18.3 MΩ·cm). Wherever the chemicals were concerned, only PTFE, glass and stainless steel were used. The saturation tank (5), the column, the phials (6) and all other relevant parts were cleaned mechanically and rinsed intensely before use. Before each run, toluene and water were mutually saturated in the stirred saturation tank in order to avoid additional mass transfer. After complete phase separation, the column is filled with water from the bottom via PTFE tubes. The toluene droplets are generated with the capillary device which allows automatic drop detachment. It consists of a hand-made glass capillary (7) which is connected with a movable inner tube to a solenoid assembly (8). A Hamilton® PSD/2 module (9) is used to generate droplets of a specified volume. The drop detachment is accomplished by the solenoid within a computer controlled sequence (10), generating a quick movement of the capillary downwards. After release, the drop rises through the continuous phase to the head of the column.

Position of Fig. 2

The rise velocity and the trajectories of the drops were obtained from a high-speed camera device. For this purposes, a Photonfocus® MV-752-160 high-speed camera (11) with a ⅔"-CMOS sensor has been used. The frame rate was set to f = 100 Hz in all investigations. The camera position is perpendicular to the column, and the entire particle path through the column can be captured. The illumination system (12) was modified compared to earlier works [6]. Two simple fluorescent lamps (P = 30W each) with low thermal radiation have been sited in an optimal distance to one another beyond the glass column. With the power supply unit Tridonic® PCA ECO, the operation frequency is 40 kHz which provides a light output independent of fluctuations in the supply voltage. With that, a constant image brightness and quality is guaranteed.

For the image analysis, the image processing tool Image-Pro Plus® 5.1 by Media Cybernetics has been used. The recorded sequence, containing the trajectory of the droplet through the column, is stored via the framegrabber on the hard disc of a computer (13). A reference frame is subtracted from each original image of the sequence, and the latter is then transformed into a binary image using a threshold value. Complete image processing results in a table with the vertical and horizontal position (x and y coordinates respectively) of the mass centre of the drop for each frame. The rise velocity and the deviation from the column axis can then be calculated.

2.2 Performed experiments

Both mass transfer directions of acetone were investigated. If the mass transfer direction is from the dispersed to the continuous phase ($d \rightarrow c$), the initial solute concentration in the toluene sample is $c_{s,0}$ whereas the solute concentration in the continuous phase is zero. When the mass transfer direction is inverted ($c \rightarrow d$), the continuous phase is enriched with acetone in the saturation tank in order to guarantee

This is an preprint of an article published in International Journal of Heat and Mass Transfer 52 (11-12) 2543-2551 (2009).
DOI: http://dx.doi.org/10.1016/j.ijheatmasstransfer.2008.11.022. © copyright 2009 Elsevier Ltd.

a homogeneous distribution of acetone in the continuous phase and then given into the column. The initial solute concentration is labelled $c_{s,0}$, and the toluene drop is then initially free of solute. Table 1 shows the investigated initial solute concentrations for both mass transfer directions.

Position of Table 1

A sufficient number of sequences were conducted for every initial concentration and diameter in order to guarantee statistical significance. The ratio of the initial solute concentrations $d \rightarrow c$ and $c \rightarrow d$ respectively was set equal to the distribution coefficient m:

$$\frac{c_{s,0(d\rightarrow c)}}{c_{s,0(c\rightarrow d)}} = m \qquad (1)$$

with

$$m = \left.\frac{c_{s,d}}{c_{s,c}}\right|_{r=R} \qquad (2)$$

With that, the equilibrium acetone concentration inside the drop for $t \rightarrow \infty$ in the $c \rightarrow d$ case is equal to the initial concentration for $d \rightarrow c$. This ensures that from the beginning until the end of the process the same amount of matter has been transported between both phases for the two mass transfer directions. In general, the distribution coefficient m is a function of solute concentration and temperature [26]. Experiments by Schulze [27] showed that the distribution coefficient m is constant in a predominant range of weight fractions investigated in this study ($m \approx 0.63$).

3. Results and discussion

3.1 System without mass transfer

Fig. 3 shows the drop rise velocity for the four relevant diameters as a function of time. In this case, no solute is added, toluene and water are mutually saturated so that no additional mass transfer takes place. In Fig. 3, only one sequence is shown for each diameter, but multiple investigations proved high reproducibility and thus statistical significance, see also [6]. Except for d_P = 2.5 mm, the drops accelerate immediately within one second to their constant terminal drop rise velocity. Larger drops (d_P = 2.5 mm) accelerate to a peak velocity. Thereafter, the velocity decreases and then oscillates around a lower value with dampening amplitude. Table 2 summarizes the terminal drop rise velocity v_t, Reynolds number Re and drag coefficient C_D defined by Equation (3).

$$C_D = \frac{4}{3}\frac{\rho_c - \rho_d}{\rho_c}\frac{g d_P}{v_t^2} \qquad (3)$$

Position of Fig. 3

Position of Table 2

This is an preprint of an article published in International Journal of Heat and Mass Transfer 52 (11-12) 2543-2551 (2009).
DOI: http://dx.doi.org/10.1016/j.ijheatmasstransfer.2008.11.022. © copyright 2009 Elsevier Ltd.

Previous studies [6] showed that the correlation of Hamielec et al. [28] obtained by applying Galerkin's method, see Equation (4), is quite suitable to estimate the drag coefficient for non-oscillating toluene droplets:

$$C_D = \frac{3.05\left(783\mu^{*2} + 2142\mu^{*} + 1080\right)}{\left(60 + 29\mu^{*}\right)\left(4 + 3\mu^{*}\right) \cdot Re^{0.74}} \qquad (4)$$

The drag coefficient in Equation (4) is calculated using the experimental data of the terminal drop rise velocity. The values are given in Table 2.

3.2 System with simultaneous mass transfer

3.2.1 Transient drop rise velocity

In case of simultaneous mass transfer of solute during drop rise, the fluid dynamic behaviour changes dramatically. As mentioned above, Marangoni flows develop at the interface and generate additional shear stress. As shown in a recent study by Wegener et al. [6], these additional contributions enhance the drag coefficient temporarily, and thus the drop rise velocity is transient and therefore a very sensitive indicator of Marangoni convection. Nevertheless, under certain conditions, mass transfer can be significantly enhanced when drop velocity is only slightly affected by Marangoni convection, see [6]. Depending on the initial solute concentration, the retardation effect of the droplet and its persistence can be more or less pronounced. The effect of initial solute concentration is shown in Fig. 4 for both mass transfer directions (left: $c \rightarrow d$, right: $d \rightarrow c$). The drop diameter is d_P = 2 mm. The rise velocities for a rigid sphere $v_{t,rs}$ given by Brauer & Mewes [29], Equation (5),

$$C_D = \frac{24}{Re} + \frac{4}{Re^{0.5}} + 0.4 \qquad \left(0 \le Re \le 3 \cdot 10^5\right) \qquad (5)$$

calculated together with Equation (3), and for an unloaded drop $v_{t,fi}$ calculated with Equation (4) are given for comparison (with physical properties of the binary system toluene/water). If no mass transfer takes place ($c_{s,0}$ = 0), the behaviour is identical to Fig. 3. If acetone is added, the drop is decelerated. For the two lowest concentrations, the deceleration is moderate but significant. The velocity is well below the case $c_{s,0}$ = 0. If a certain concentration is reached, the drop accelerates only to the velocity of the comparable rigid sphere, $v_{t,rs}$. This velocity seems to be the lower limit, smaller velocities have not been observed (see also [5]). In this stage, inner circulation is replaced by a chaotic flow pattern inside the whole drop.

Furthermore, Fig. 4 shows that after a certain time, the drop reaccelerates suddenly to a higher velocity. For both mass transfer directions it can be stated that the higher the initial concentration is, the later is the reacceleration. Obviously, Marangoni convection gets weaker due to ongoing mass transfer and thus smaller concentration gradients. The inner circulation can now be established since the opposing shear forces vanish.

This is an preprint of an article published in International Journal of Heat and Mass Transfer 52 (11-12) 2543-2551 (2009).
DOI: http://dx.doi.org/10.1016/j.ijheatmasstransfer.2008.11.022. © copyright 2009 Elsevier Ltd.

Position of Fig. 4

Results suggest that the reacceleration time is characteristic for each diameter and initial solute concentration. Fig. 5 shows for both mass transfer directions the drop rise velocity as a function of time for different drop diameters. The initial solute concentrations are 12 g/L ($c \rightarrow d$) and 7.5 g/L ($d \rightarrow c$) respectively. Again, only one sequence is shown for convenience, the reproducibility has been verified. For all diameters and both mass transfer direction it can be seen that the velocity of the rigid sphere is attained after the first acceleration. Reacceleration occurs the later the smaller the droplet is. It is interesting to note that even for the smallest diameter (d_P = 1 mm) a reacceleration can be observed. This indicates that even drops down to this size small have a significant inner circulation and thus cannot be regarded as rigid.

If both mass transfer directions are compared it can be noticed that the reacceleration is more distinct in the $c \rightarrow d$ case. The slope of the velocity curve for the direction $d \rightarrow c$ is flatter. The reacceleration takes place significantly later if the corresponding cases are compared. Additionally, it seems that the drop rise velocity slowly increases continuously whereas for $c \rightarrow d$, the drop rise velocity stays more or less constant until reacceleration. It is noticeable that the maximum velocities and the oscillating amplitudes are higher in the case $c \rightarrow d$ for all diameters.

For the other concentrations not shown here the behaviour is qualitatively equal. The general statement that reacceleration is the later the higher the initial concentration was is valid for all investigated drop diameters. Further on, if the initial solute concentration is below a certain critical value, Marangoni convection is too weak to decelerate the drop on the velocity level of a rigid sphere but too strong than the velocity would be comparable to the case without mass transfer.

Position of Fig. 5

3.2.2 Particle trajectories

The particle trajectories reveal interesting details. Fig. 6 shows a representative example of more than ten rising paths of 2 mm droplets for both mass transfer directions. The initial solute concentrations are the same as in Fig. 5. After release from the capillary tip, the drops rise vertically on a straight line. This stage corresponds to the time interval where the rise velocity is that of a rigid sphere. For the mass transfer direction $c \rightarrow d$, Fig. 5a, the scatter in the horizontal coordinate is noticeable smaller than in the reversed direction.

At reacceleration time, there is a significant change in the fluid dynamic behaviour of the droplets. For $c \rightarrow d$, the drops start to oscillate around the vertical axis on a wiggly line, but they stay close to the vertical column axis. For the reversed mass transfer direction $d \rightarrow c$, the drops suddenly break out from the centre of the column, tend toward the column wall and move back again. The displacement direction is arbitrary. In the experiments, there were both drops drifting to the column wall remaining in this area, and drops with lateral movement of higher amplitude returning to the centre of the column.

If Fig. 6 is compared with Figs. 4 & 5, one can see that the two effects reacceleration and drop displacement happen at the same time. The behaviour shown in Fig. 6 is qualitatively the same for the other cases not shown here. According to the reacceleration, the drop displacement is the earlier the lower

This is an preprint of an article published in International Journal of Heat and Mass Transfer 52 (11-12) 2543-2551 (2009).
DOI: http://dx.doi.org/10.1016/j.ijheatmasstransfer.2008.11.022. © copyright 2009 Elsevier Ltd.

the initial concentration is for both mass transfer directions. If the initial concentration is below a certain value (i.e. < 3.7 g/L for $d \rightarrow c$ and < 5.9 g/L for $c \rightarrow d$), there is no first velocity plateau and thus no distinct point of reacceleration. In fact, the drops start to oscillate or to break out directly after their release from the capillary.

Position of Fig. 6

For other drop sizes, the fluid dynamic behaviour is qualitatively the same. For oscillating droplets (i.e. d_P = 2.5 mm), it is interesting to note that Marangoni effects seem to stabilise the drop rising path compared with the case without mass transfer. When there is no mass transfer, the velocity of bigger droplets starts to oscillate directly after the first acceleration (see Fig. 3). In the case of additional mass transfer, the velocity remains stable for a longer period of time. After reacceleration however, the velocity oscillation can be established.

The influence of the mass transfer direction on the fluid dynamic behaviour is obvious in Fig. 6. In the direction $c \rightarrow d$, the path is stabilised in a sense that the main direction stays vertically upward, whereas for $d \rightarrow c$, the drops break out with significant lateral movements with higher amplitude compared to $c \rightarrow d$. Since the change in fluid dynamics appears shortly after reacceleration, the way how the inner circulation is reinitiated is possibly of great importance. Two possible mechanisms are proposed in Fig. 7 (a-c) for both mass transfer directions. When Marangoni effects are strong, internal circulation is hindered due to local convection patterns initiated by the movement of the interface. The drop rise velocity is that of a rigid sphere (Fig. 7a). The reacceleration starts when the opposing shear stresses due to Marangoni convection decrease and the internal circulation patterns develop. In the case $c \rightarrow d$, according to Fig. $7b_1$, a higher order of symmetry must occur, i.e. that pressure gradients are quickly equalized and the drop oscillates with relatively small deviation. For $d \rightarrow c$ (Fig. $7b_2$), the order of symmetry is lower, the internal circulation develops in a certain section of the drop whereas in the rest of the drop Marangoni flows are still active. Thus, the interfacial velocity distribution along the drop surface is unequal and pressure gradients must consequently occur, since only normal forces can lead to a lateral motion. At the end of the process, when mass transfer is completed and all concentration gradients are zero, full internal circulation is developed in both cases (Fig. 7c).

Position of Fig. 7

3.2.3 Correlation of results

One main objective of this study is to characterize the duration of Marangoni convection dominance. The results presented above showed that the drop rise velocity can significantly be retarded which of course affects the residence time of the dispersed phase. The evolution of the transient drop rise velocity depends mainly on the parameters drop diameter, initial solute concentration and mass transfer direction. It can generally be found that a two-step acceleration behaviour appears if the initial solute concentration is high enough to decelerate the droplet to the velocity of a comparable rigid sphere. After a certain time, the reacceleration takes place. Results reveal that the reacceleration time is the later the higher the initial concentration and the smaller the droplet diameter are.

This is an preprint of an article published in International Journal of Heat and Mass Transfer 52 (11-12) 2543-2551 (2009).
DOI: http://dx.doi.org/10.1016/j.ijheatmasstransfer.2008.11.022. © copyright 2009 Elsevier Ltd.

For the following analysis, only cases showing the above mentioned two-step acceleration behaviour were considered, these were in detail the following:

$c \rightarrow d$ (22 cases in total):	all cases	for $d_P = 1$ mm
	$c_{s,0} \geq 2.9$ g/L	for $d_P = 1.5$ mm
	$c_{s,0} \geq 5.9$ g/L	for $d_P = 2$ mm
	$c_{s,0} \geq 12$ g/L	for $d_P = 2.5$ mm
$d \rightarrow c$ (24 cases in total):	all cases	for $d_P < 2$ mm
	$c_{s,0} \geq 1.9$ g/L	for $d_P = 2$ mm
	$c_{s,0} \geq 3.7$ g/L	for $d_P = 2.5$ mm

Fig. 8 shows the reacceleration time as a function of $1/c_{s,0}$ for the mass transfer direction $c \rightarrow d$ (Fig. 8a) and $d \rightarrow c$ (Fig. 8b) for all diameters investigated. All data can be fitted satisfactorily with a correlation coefficient $R^2 > 0.98$. Fig. 8 shows - according to the results shown above - that the higher the concentration and the smaller the droplet is, the higher is the reacceleration time. Qualitatively, we explain this behaviour in the following way: Reacceleration is only possible if the Marangoni induced shear forces acting on the drop become too weak to retard the drop. For a given diameter, the relevant shear forces are constant. For larger drops, the buoyancy forces increase with drop volume, and thus higher Marangoni induced shear forces are necessary to decrease drop velocity. Hence, the reacceleration can begin with higher absolute values of the shear forces. If a critical solute concentration is supposed below which Marangoni induced shear forces become irrelevant for the drop rise velocity, higher mean concentrations are permitted to allow for reacceleration. This occurs at smaller mass transfer times for bigger than for smaller particles. In addition, the mass transfer rate is lower for smaller droplets since the Reynolds number is significantly smaller. In larger droplets, chaotic flow patterns generated by the Marangoni effect can develop more intensely and thus promote the radial mixing. This possibly leads to faster mass transfer rates which in turn result in earlier reacceleration times. The observation that reacceleration is later if initial concentration is higher for a given diameter is certainly due to the fact that Marangoni convection is dominant for a longer period of time if $c_{s,0}$ is high. A critical absolute concentration value is simply reached later.

In Fig. 8, it is noticeable that there is a limit of the reacceleration time for high initial concentrations or $1/c_{s,0} \rightarrow 0$ respectively. That would mean that the reacceleration time is never higher than approximately 10 seconds, regardless of the drop diameter. Obviously, for $1/c_{s,0} \rightarrow 0$, Marangoni convection is so strong that concentration gradients are equalised in the same amount of time, or in other words the critical concentration at which reacceleration starts is reached simultaneously regardless of the drop diameter.

Position of Fig. 8

This is an preprint of an article published in International Journal of Heat and Mass Transfer 52 (11-12) 2543-2551 (2009).
DOI: http://dx.doi.org/10.1016/j.ijheatmasstransfer.2008.11.022.

A surprising fact is shown in Fig. 9. If the reacceleration time is expressed as a function of $d_P/c_{s,0}$ for the mass transfer direction $c \rightarrow d$ (Fig. 9a), all data can be brought into one single curve. In the $d \rightarrow c$ case (Fig. 9b), the best results were obtained if the reacceleration time is plotted as a function of $d_P^3/c_{s,0}$. The correlation coefficient in this case is worse than for $c \rightarrow d$ but still satisfactory ($R^2 = 0.9$ instead of 0.98).

The surprisingly good correlation provokes an attempt to model the reacceleration time. A reliable and physically meaningful model should include the parameters time, drop diameter, instantaneous drop velocity, mean solute concentration at reacceleration time and the relevant physical properties. In some way, Marangoni convection has to be considered, probably using some kind of Marangoni number including the gradient of interfacial tension at a specified time and the absolute value of the initial solute concentration. Several attempts have been made using well known mass transfer correlations [23, 30, 31] assuming a constant critical mean solute concentration at reacceleration time for the mass transfer direction $d \rightarrow c$ following [6]. For the mass transfer direction $c \rightarrow d$ however, the equilibrium concentration changes with initial concentration, so prediction of mean drop concentration at reacceleration time is impossible up to now. In any case, the correlation was unsatisfactory and implies the need for experimental results of the mean solute concentration at reacceleration time for both mass transfer directions. To be even more precise, local effects at the interface have to be incorporated into a reliable model, namely the interfacial tension gradient and the local interfacial concentration. These information are experimentally not accessible, and thus CFD methods have to be applied (see e.g. [32]).

Anyway, with Fig. 9, a graphical prediction of the end of Marangoni convection dominance for any given ratio $d_P/c_{s,0}$ and $d_P^3/c_{s,0}$ respectively is possible in the above specified parameter range. The application range of the figure could possibly be extended to higher ratios using larger drops, but droplet deformations will play a more significant role in these cases. This will be verified in future works.

Position of Fig. 9

4. Summary and conclusion

Extensive investigations of the hydrodynamic behaviour in the system toluene$_{(d)}$/acetone$_{(s)}$/water$_{(c)}$, a system which is known to show interfacial convections, have been accomplished. The drop rise velocities and the particle trajectories were analysed using high-speed photography. The investigated parameters were the drop diameter, the initial solute concentration and the mass transfer direction. Results showed that the drop rise velocity is of transient nature if Marangoni convection occurs. The additional shear stress increases temporarily the global drag coefficient so that the drop is decelerated. The higher the concentration is, the lower is the velocity, but never lower than for a rigid sphere with the same physical properties. At a certain point, a second acceleration appears which reflects the end of Marangoni convection dominance and the initialisation of the inner circulation and therewith the decrease of the drag coefficient. In general, the time of reacceleration is the earlier the lower the initial concentration is for a given diameter, and the time of reacceleration is the earlier the bigger the droplet is for a given initial solute concentration. Below a certain concentration, no distinct reacceleration was observed. The reacceleration time can be expressed as a function of the quotient of diameter and initial solute

concentration (for the mass transfer direction $c \rightarrow d$) or as a function of the quotient of volume and initial solute concentration (for the mass transfer direction $d \rightarrow c$) with satisfactory accuracy.

The behaviour of the drop rise velocity was qualitatively the same for both mass transfer directions. Interesting differences were observed in terms of the particle trajectories. Marangoni convection is able to stabilise the rising path until reacceleration begins, especially for larger droplets. In case of reacceleration, if the mass transfer direction is from the continuous to the dispersed phase, the droplets oscillate around their vertical rise axis, whereas in the opposite mass transfer direction the drops break out laterally.

For accurate modelling of the present results, the mean solute concentration at reacceleration time is needed. Up to now, these experimental data only exist for one diameter and one mass transfer direction. The correlation of mass transfer measurements with fluid dynamic investigations has been shown exemplarily for one droplet diameter and one mass transfer direction in [6]. Future works will consider the associated mass transfer measurements for the parameter range investigated in this study

The presented strategy to characterise the duration and effect of Marangoni convection can be applied to other systems in order to investigate the dependence of the results on physical properties e.g. the viscosity ratio, ratio of diffusion coefficients or distribution coefficient.

Acknowledgement

Financial support provided by the German Research Foundation (DFG) is gratefully acknowledged.

References

[1] L. Steiner, G. Oezdemir, S. Hartland (1990). Single-Drop Mass Transfer in the Water-Toluene-Acetone System, Ind. Eng. Chem. Res., 29, 1313-1318.

[2] H. Sawistowski, Surface-tension-induced interfacial convection and its effect on rates of mass transfer, Chemie Ingenieur Technik 45 (18) (1973) 1093-1098.

[3] C.V. Sternling, L.E. Scriven, Interfacial turbulence: hydrodynamic instability and the Marangoni effect, AIChE Journal 5 (4) (1959) 514-523.

[4] M. Henschke, Auslegung pulsierter Siebboden-Kolonnen. Habilitation, Fakultät für Maschinen-wesen, RWTH Aachen, 2004.

[5] K. Schulze, M. Kraume, Influence of Mass Transfer on Drop Rise Velocity, in: Schindler, F.-P. (Ed.), 1st International Berlin Workshop - IBW1 on Transport Phenomena with Moving Boundaries, Berlin, 2001.

[6] M. Wegener, A.R. Paschedag, M. Kraume, Transient Rise Velocity and Mass Transfer of a Single Drop with Interfacial Instabilities - Experimental Investigations, Chemical Engineering Science 62 (11) (2007) 2967-2978.

[7] S. Hu, R.C. Kintner, The fall of single liquid drops through water, AIChE Journal 1 (1) (1955) 42-48.

[8] A.I. Johnson, L. Braida, The velocity of fall of circulating and oscillating liquid drops through quiescent liquid phases, The Canadian journal of chemical engineering 35 (1957) 165-172.

[9] W. Licht, G.S.R. Narasimhamurty, Rate of Fall of Single Liquid Drops, AIChE Journal 1 (3) (1955) 366-373.

[10] G. Thorsen, R.M. Stordalen, S.G. Terjesen, On the terminal velocity of circulating and oscillating liquid drops, Chemical Engineering Science 23 (5) (1968) 413-426.

[11] R.M. Edge, C.D. Grant, The motion of drops in water contaminated with a surface-active agent, Chemical Engineering Science 27 (9) (1972) 1709-1721.

[12] R.M. Griffith, The effect of surfactants on the terminal velocity of drops and bubbles, Chemical Engineering Science 17 (12) (1962) 1057-1070.

[13] L. Mekasut, J. Molinier, H. Angelino, Effects of surfactants on mass transfer outside drops, Chemical Engineering Science 33 (7) (1978) 821-829.

[14] K. E. Spells, A Study of Circulation Patterns within Liquid Drops moving through a Liquid, Proceedings of the Physical Society. Section B 65 (7) (1952) 541.

[15] A. Amar, E. Groß-Hardt, A.A. Khrapitchev, S. Stapf, A. Pfennig, B. Blümich, Visualizing flow vortices inside a single levitated drop, Journal of Magnetic Resonance 177 (1) (2005) 74-85.

[16] F. H. Garner, A. H. P. Skelland, Some factors affecting droplet behaviour in liquid-liquid systems, Chemical Engineering Science 4 (4) (1955) 149-158.

[17] A.J. Klee, R.E. Treybal, Rate of rise or fall of liquid drops, AIChE Journal 2 (4) (1956) 444-447.

[18] E.R. Elzinga, J.T. Banchero, Some observations on the mechanics of drops in liquid-liquid systems, AIChE Journal 7 (3) (1961) 394-399.

[19] S. Winnikow, B.T. Chao, Droplet Motion in Purified Systems, Physics of Fluids 9 (1) (1966) 50-61.

[20] F. W. Keith, A. N. Hixson, Liquid-Liquid Extraction Spray Columns-Drop formation and interfacial transfer area, Industrial and Engineering Chemistry 47 (2) (1955) 264-266.

[21] T. Al-Hassan, C.J. Mumford, G.V. Jeffreys, Flow characteristics of large oscillating drops in liquid-liquid systems, Chemical Engineering & Technology 14 (1) (1991) 65-72.

[22] H. Linde, B. Sehrt, Der Einfluss der Marangoni-Instabilität auf den hydrodynamischen Widerstand der Tropfen im System Benzaldehyd-Essigsäure-Wasser, Zeitschrift für physikalische Chemie München 231 (3-4) (1966) 151-172.

[23] M. Henschke, A. Pfennig, Mass-Transfer Enhancement in Single-Drop Extraction Experiments, AIChE Journal 45 (10) (1999) 2079-2086.

[24] D. Garthe, Fluiddynamics and Mass Transfer of Single Particles and Swarms of Particles in Extraction Columns, PhD thesis, Fakultät für Maschinenwesen, TU München, 2006.

[25] T. Misek, R. Berger, J. Schröter. Standard test systems for liquid extraction, Inst. Chem. Eng., EFCE Publication Series, 46 (1985).

[26] W.J. Korchinsky, C.H. Young, High flux mass transfer: Comparison of liquid-liquid extraction column and drop (Handlos-Baron) model predictions with rotating disc contactor performance, Chemical Engineering Science 41 (12) (1986) 3053-3061.

[27] Schulze, K. (2007). Stoffaustausch und Fluiddynamik am bewegten Einzeltropfen unter dem Einfluss von Marangonikonvektion. PhD Thesis, Fachgebiet Verfahrenstechnik, TU Berlin

[28] A.E. Hamielec, S.H. Storey, J.M. Whitehead, Viscous flow around fluid spheres at intermediate Reynolds-numbers, Canadian Journal Chem. Eng. 12 (1963) 246-251.

[29] H. Brauer, D. Mewes, Strömungswiderstand sowie stationärer und instationärer Stoff- und Wärmeübergang an Kugeln, Chemie Ingenieur Technik 44 (13) (1972) 865-868.

[30] R. Kronig, J.C. Brink, On the Theory of Extraction from Falling Droplets, Applied Scientific Research Section a-Mechanics Heat Chemical Engineering Mathematical Methods 2 (2) (1950) 142-154.

[31] P.H. Calderbank, I.J.O. Korchinski, Circulation in liquid drops: (A heat-transfer study), Chemical Engineering Science 6 (2) (1956) 65-78.

[32] A.R Paschedag, M. Wegener, Three-dimensional simulations of mass transfer at single droplets, Proceedings of the Fifth International Conference on Computational Fluid Dynamics in the Process Industries, CSIRO Australia, ISBN: 0 643 09423 7 (2006).

This is an preprint of an article published in International Journal of Heat and Mass Transfer 52 (11-12) 2543-2551 (2009).
DOI: http://dx.doi.org/10.1016/j.ijheatmasstransfer.2008.11.022.

Figure captions

Fig. 1: Scheme of the development of interfacial flows induced by interfacial tension gradients. σ_{hi}: zone of higher interfacial tension, σ_{lo}: zone of lower interfacial tension.

Fig. 2: Experimental setup for the measurement of transient drop rise velocities. (1) column, (2) jacket, (3) gear pump, (4) thermostat, (5) saturation tank, (6) sample, (7) capillary device, (8) solenoid device, (9) Hamilton pump, (10) computer control, (11) high-speed camera, (12) illumination system, (13) data collecting and image processing.

Fig. 3: Drop rise velocity of toluene drop in water (mutually saturated) as a function of time for different drop diameters. No solute was added. The terminal velocities calculated with the model of Hamielec et al. [28] are given for comparison (− · − curves).

Fig. 4: Drop rise velocity as a function of time for different initial solute concentrations. Drop diameter d_P = 2 mm. (a) mass transfer direction *c*→*d.* (b) *d*→*c.*

Fig. 5: Drop rise velocity as a function of time for different drop diameters. (a) mass transfer direction *c*→*d,* $c_{s,0}$ = 12 g/L. (b) *d*→*c*, $c_{s,0}$ = 7.5 g/L. The velocity levels for the corresponding rigid spheres are given for comparison.

Fig. 6: Particle trajectories of 2 mm droplets. (a) mass transfer direction *c*→*d*, $c_{s,0}$ = 12 g/L. (b) *d*→*c* $c_{s,0}$ = 7.5 g/L.

Fig. 7: Scheme of inner circulation pattern. a: fully developed Marangoni convection. b_1: onset of symmetric inner circulation (*c*→*d*). b_2: onset of asymmetric inner circulation (*d*→*c*). c: inner circulation without Marangoni convection.

Fig. 8: Reacceleration time as a function of $1/c_{s,0}$ for different drop diameters. (a) mass transfer direction *c*→*d.* (b) *d*→*c.*

Fig. 9: Reacceleration time as a function of the ratio $d_P/c_{s,0}$ for the mass transfer direction *c*→*d* (a), and as a function of the ratio $d_P^3/c_{s,0}$ for *d*→*c* (b).

This is an preprint of an article published in International Journal of Heat and Mass Transfer 52 (11-12) 2543-2551 (2009).
DOI: http://dx.doi.org/10.1016/j.ijheatmasstransfer.2008.11.022. © copyright 2009 Elsevier Ltd.

Tables

Table 1: Performed measurements

d_P = 1, 1.5, 2, 2.5 mm	
$d \rightarrow c$: $c_{s,0}$ [g/L]	$c \rightarrow d$: $c_{s,0}$ [g/L]
0.9	1.4
1.8	2.9
3.7	5.9
7.5	12
15	24
30	49
60	95

Table 2: Terminal drop rise velocities v_t, Re and C_D

d_P [mm]	1	1.5	2	2.5_{peak}	$2.5_{osc.}$
v_t [mm/s]	35	65	105	145	115
Re	39	109	235	406	322
C_D	1.44	0.63	0.32	0.33	0.21
C_D (Hamielec et al.)	1.2	0.56	0.32	0.21	0.25

This is an preprint of an article published in International Journal of Heat and Mass Transfer 52 (11-12) 2543-2551 (2009).
DOI: http://dx.doi.org/10.1016/j.ijheatmasstransfer.2008.11.022.

Figures

Figure 1:

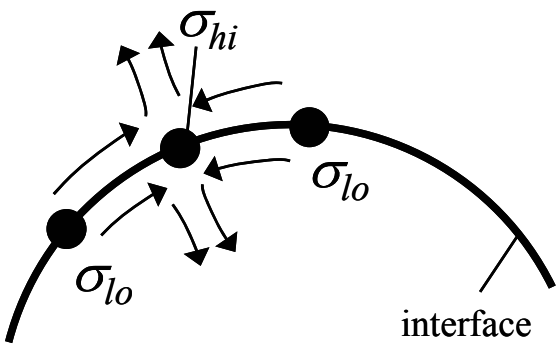

This is an preprint of an article published in International Journal of Heat and Mass Transfer 52 (11-12) 2543-2551 (2009).
DOI: http://dx.doi.org/10.1016/j.ijheatmasstransfer.2008.11.022. © copyright 2009 Elsevier Ltd.

Figure 2:

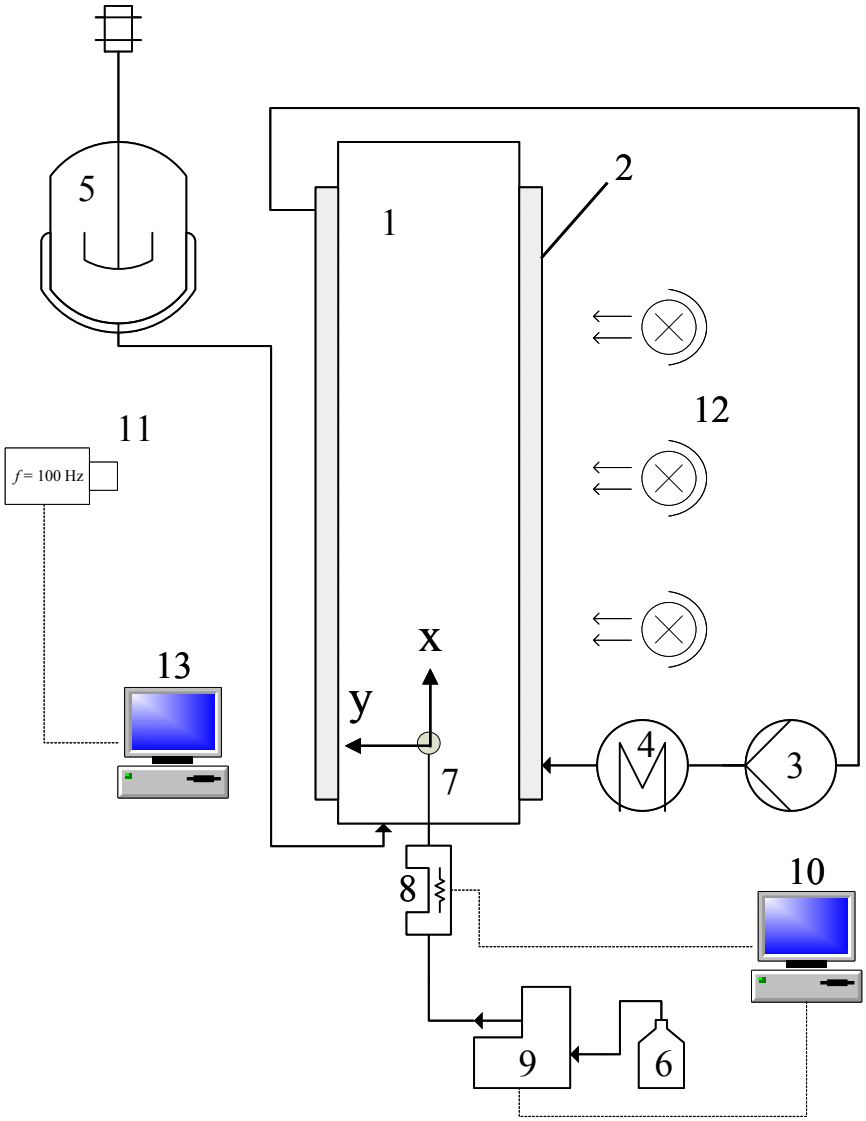

This is an preprint of an article published in International Journal of Heat and Mass Transfer 52 (11-12) 2543-2551 (2009).
DOI: http://dx.doi.org/10.1016/j.ijheatmasstransfer.2008.11.022. © copyright 2009 Elsevier Ltd.

Figure 3:

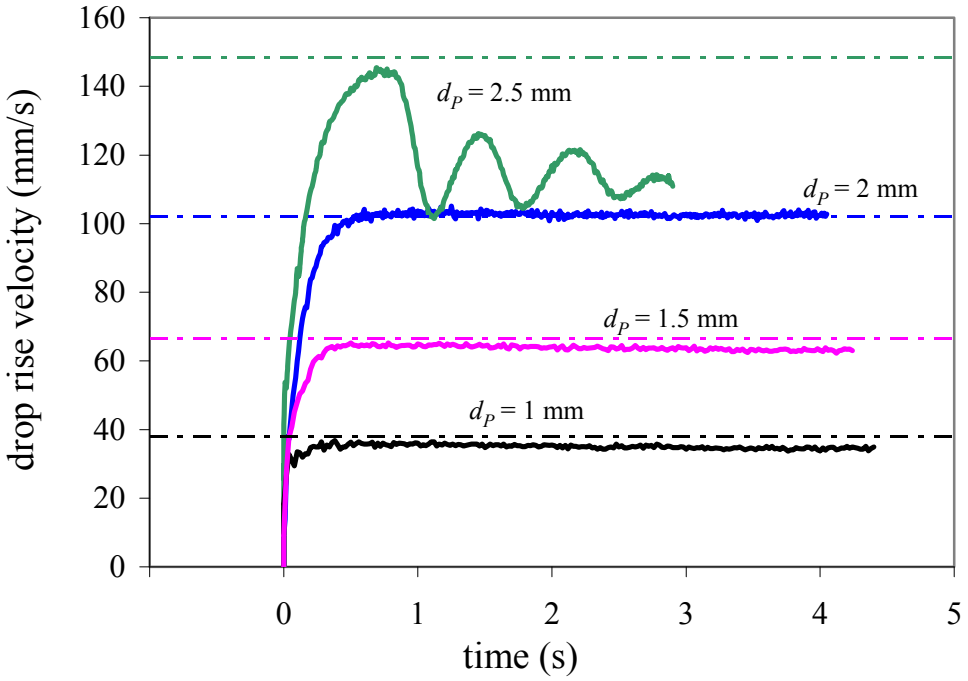

This is an preprint of an article published in International Journal of Heat and Mass Transfer 52 (11-12) 2543-2551 (2009).
DOI: http://dx.doi.org/10.1016/j.ijheatmasstransfer.2008.11.022. © copyright 2009 Elsevier Ltd.

Figure 4:

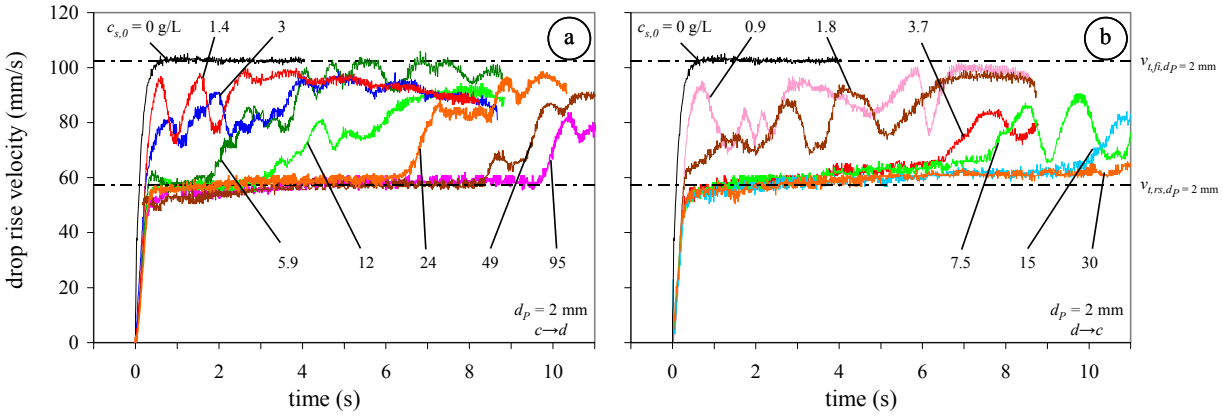

This is an preprint of an article published in International Journal of Heat and Mass Transfer 52 (11-12) 2543-2551 (2009).
DOI: http://dx.doi.org/10.1016/j.ijheatmasstransfer.2008.11.022. © copyright 2009 Elsevier Ltd.

Figure 5:

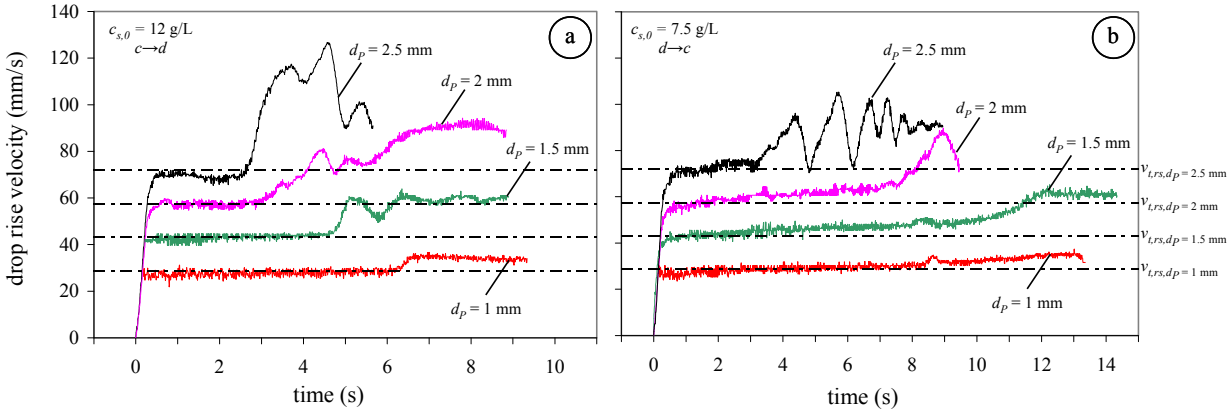

This is an preprint of an article published in International Journal of Heat and Mass Transfer 52 (11-12) 2543-2551 (2009).
DOI: http://dx.doi.org/10.1016/j.ijheatmasstransfer.2008.11.022. © copyright 2009 Elsevier Ltd.

Figure 6:

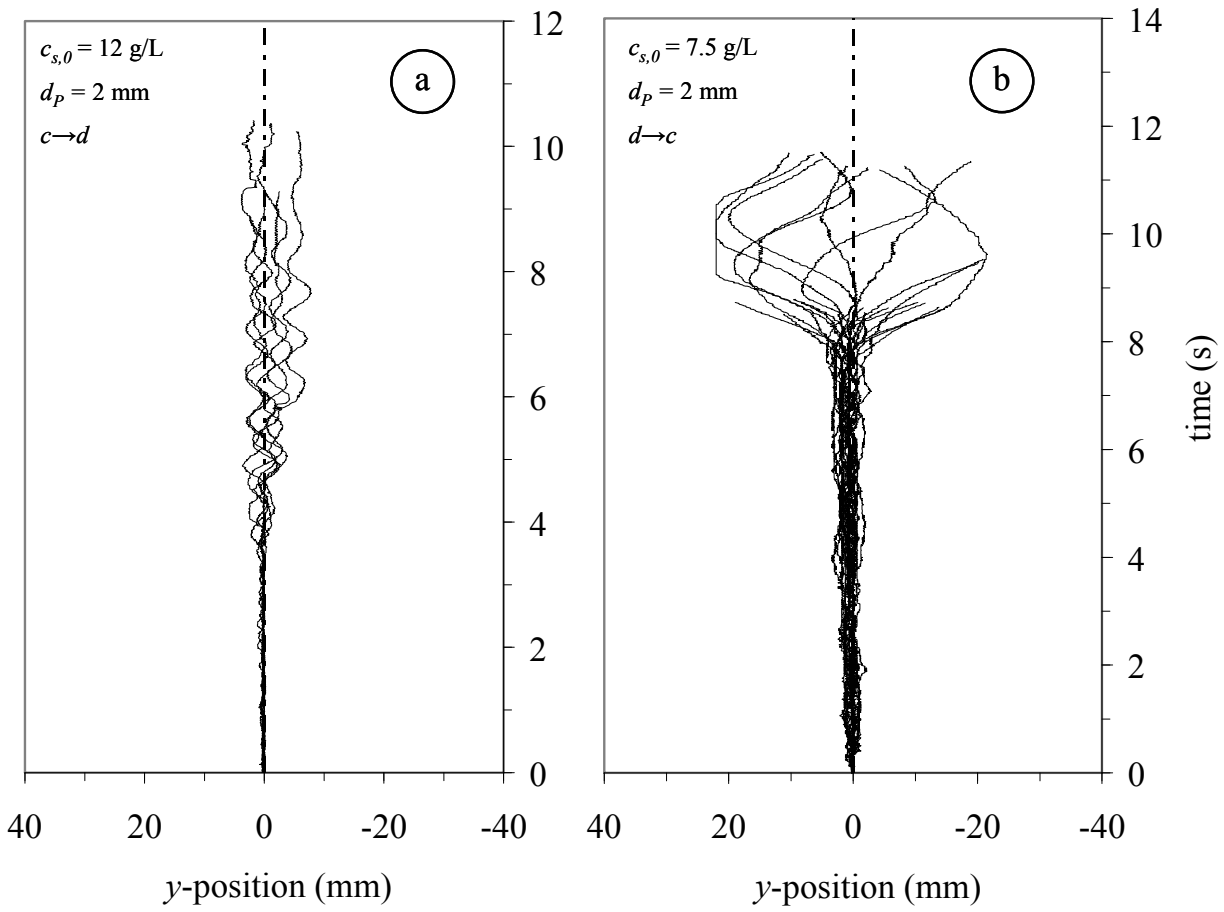

This is an preprint of an article published in International Journal of Heat and Mass Transfer 52 (11-12) 2543-2551 (2009).
DOI: http://dx.doi.org/10.1016/j.ijheatmasstransfer.2008.11.022. © copyright 2009 Elsevier Ltd.

Figure 7:

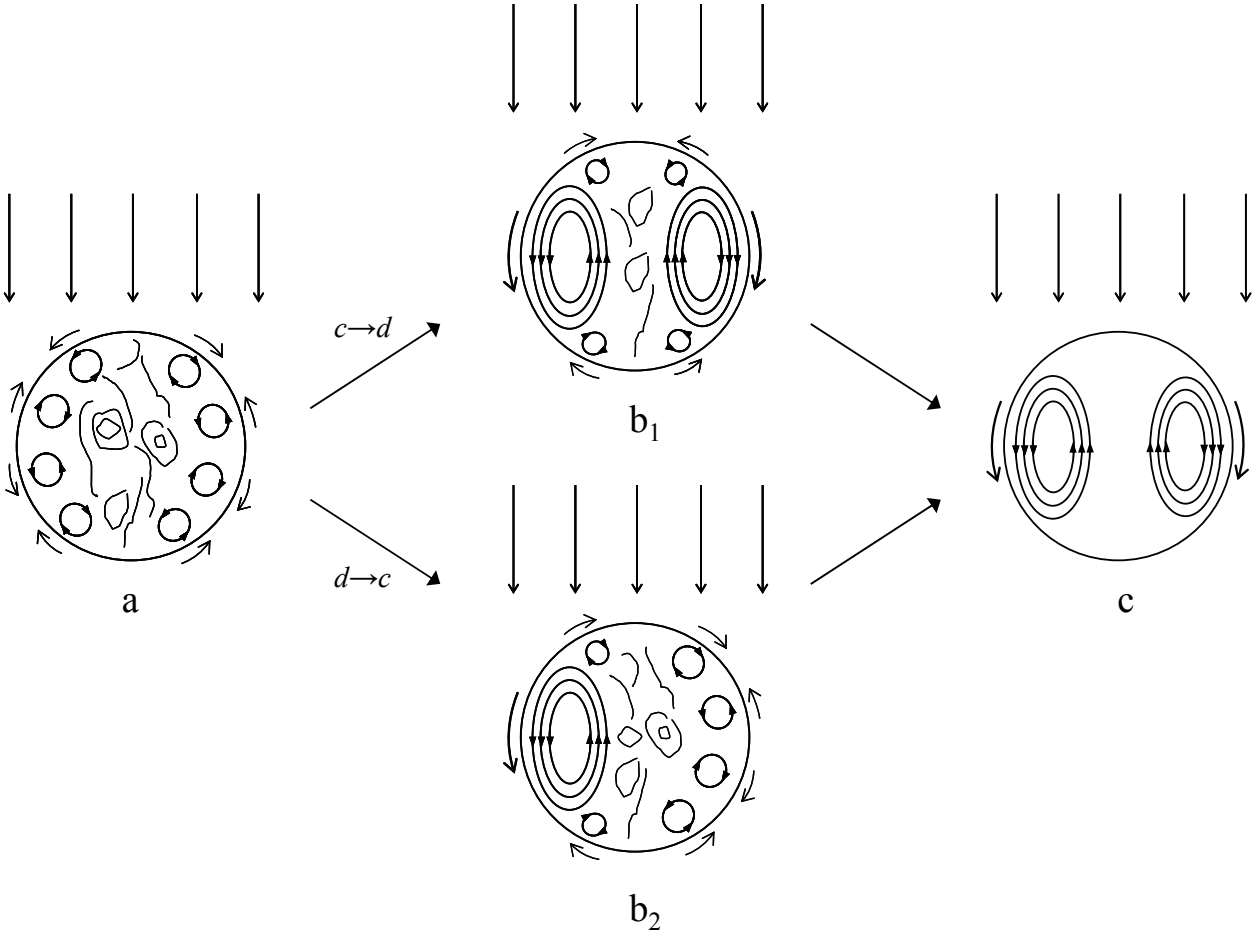

This is an preprint of an article published in International Journal of Heat and Mass Transfer 52 (11-12) 2543-2551 (2009).
DOI: http://dx.doi.org/10.1016/j.ijheatmasstransfer.2008.11.022. © copyright 2009 Elsevier Ltd.

Figure 8:

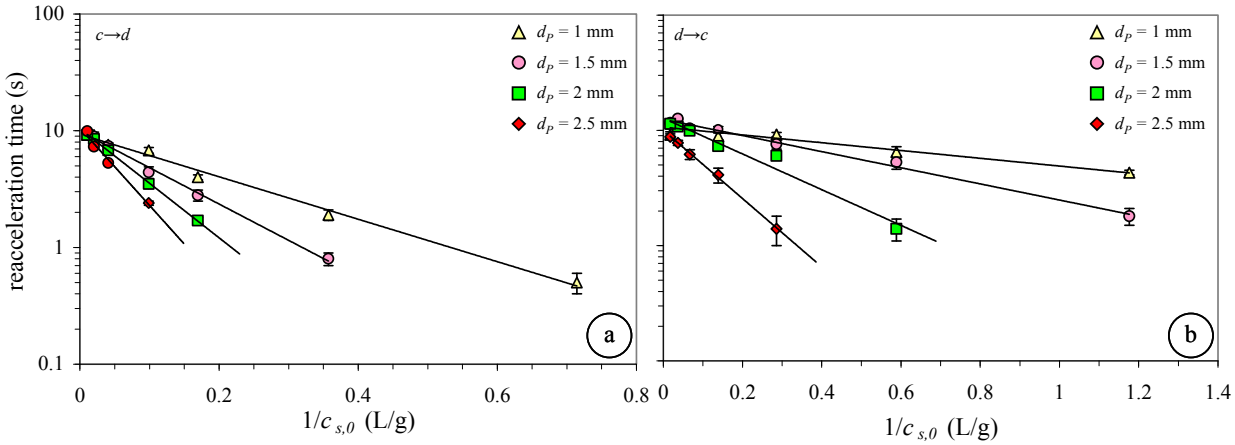

This is an preprint of an article published in International Journal of Heat and Mass Transfer 52 (11-12) 2543-2551 (2009).
DOI: http://dx.doi.org/10.1016/j.ijheatmasstransfer.2008.11.022. © copyright 2009 Elsevier Ltd.

Figure 9: